Applied Biological Research 26(1): 33-42; (2024)
DOI: 10.48165/abr.2024.26.01.4

GREEN SYNTHESIS OF THREE UNIQUE NANOPARTICLES FROM *Hibiscus Ficulneus* L. AND ASSESSMENT OF THEIR POTENTIAL ANTIMICROBIAL PROPERTIES

Antony Selvi Albert Raja[1], Nelson Samuel Jebastin[2], Ilango Kaliappan[3] and Nalini Ramachandran[4]

[1]*Department of Botany, St. Mary's College (Autonomous), Thoothukudi - 628 002, Tamil Nadu (India)*
[2]*Department of Zoology, Annamalai University, Annamalainagar, Chidambaram- 608 002, Tamil Nadu (India)*
[3]*School of Pharmacy, Hindustan Institute of Technology and Science, Padur, Chennai – 603 103, Tamil Nadu (India)*
[4]*Department of Applied Sciences, Chemistry Section University of Technology and Applied Sciences, Muscat (Sultanate of Oman)*
*****e-mail: *selvi2438@gmail.com*

(Received 17 September, 2023; accepted 26 December, 2023)

ABSTRACT

The synthesis and characterization of various nanoparticles using the extracts from *Hibiscus ficulneus* L., a medicinal plant known for its therapeutic properties, were investigated. Nanoparticles of three metals, namely silver, copper and zinc (used in the form of silver nitrate, copper sulphate, and zinc sulphate) were synthesized. The presence of nanoparticles was confirmed by observing a spectrum in visible range, which was carried out using a UV-visible spectrophotometer. To observe the crystalline structure, XRD analysis was performed. SEM analysis revealed uniformly distributed silver nanoparticles on the surfaces of the cells. The silver nanoparticles were spherical in shape with particle size in the range of 2 to 20 µm. The antimicrobial activity of the synthesized nanoparticles was evaluated using the zone of inhibition method. The highest antimicrobial activity was observed with silver nanoparticles as compared to the other silver nano-particle extracts, particularly against *Pseudomonas aeruginosa* (20 mm). These results highlight the significant antimicrobial potential of silver nanoparticles against pathogenic bacteria. This study underscores the role of terrestrial products as potential sources for pharmaceutical applications.

Keywords: Antimicrobial activity, *Hibiscus ficulneus*, nanoparticles, SEM, XRD

INTRODUCTION

Plants synthesize a wide variety of chemical compounds which are involved in essential bio-logical functions and/or defence against predators. The organic molecules found in these plants can serve as models for synthetic drugs. Approximately 10% vascular plants possess medicinal properties (Fonnegra, 2007) and as per the conservative estimates worldwide there are 350,000-500,000 medicinal plant species (Joppa *et al.,* 2011; Pimm *et al.,*2014). In India, around 20,000 medicinal plants have been recorded, although traditional practitioners use only about 7500 plants for various disease treatments. In India about 7800 manufacturing units are engaged in producing natural health products and traditional plant-based formulations, which annually require over 2000 t raw

medicinal plant materials (Pandey *et al.*, 2008). Additionally, over 1500 herbal products are sold as dietary supplements or ethnic traditional medicines (Patwardhan *et al.*, 2005).

The synthesis of nanoparticles of 1 to 100 nm size have found applications in medicinal chemistry, atomic physics, and various biological fields (Murugan and Shanmugasundaram, 2014). Nanomaterials, the atomic and molecular building blocks (approximately 0.2 nm) of matter, exist in amorphous or crystalline forms, and their surfaces can serve as carriers for liquid droplets or gases (Buzea *et al.,* 2007). Characterization of nanoparticles involves examining their size, shape, and quantity. The various techniques used for characterization include UV-visible spectroscopy, X-ray diffraction (XRD), and scanning electron microscopy (SEM), etc. Nanoparticles have generated significant interest due to their extremely small size and large surface-to-volume ratio, which impart them unique properties in comparison to the bulk materials. The nanoparticles have gained importance in biomedicine and bioremediation, especially in drug and gene delivery, cancer therapy, disease diagnostic, bioengineering, biosensors, etc. (Kavitha *et al.,* 2013; Yuan *et al.*, 2016).

Biological nanoparticles can be synthesized by using bacteria, fungi, and plants. Biological methods, also known as green synthesis approach to nanoparticle production have the potential to replace physical and chemical methods due to their economic and ecological sustainability (Baishya *et al.,* 2012). Plants, renowned for their therapeutic value, are capable of biologically synthesizing nanoparticles, which find applications in various fields. Since silver and zinc oxide nanoparticles have antibacterial capabilities, so using them as a preventative measure against infectious diseases is considered a possible viable option. Size, shape, composition, crystallinity, and morphology are the primary determinants of metal nanoparticle's intrinsic attributes (Dickson *et al.,* 2000). Silver is currently gaining popularity among metal nanoparticles due to its improved features. The particle size at the nanoscale level results in a large surface area per mass where a large number of atoms are in immediate touch and ready for reaction. The experimental circumstances have a substantial influence on size, shape, stability, and characteristics (chemical and physical) of metal nanoparticles. In light of above, the current study was aimed to synthesize and analyse nanoparticles mediated by *Hibiscus ficulneus* as well as assess their antimicrobial properties against some selected pathogenic microbes.

MATERIALS AND METHODS

Collection of plant material

Hibiscus ficulneus L., an angiospermic plant selected for the present study, was collected from the campus of G. Venkataswamy Naidu College, Kovilpatti, Thoothukudi district, Tamil Nadu (India) and its identity was got authenticated by the botanical experts in the college. The fresh and healthy plant materials were thoroughly rinsed with tap water, followed by distilled water to remove all dirt and dust.

Synthesis of nanoparticles

The whole fresh plants of *H. ficulneus* (10 g) were boiled in 100 mL double-distilled water for 4 h, then filtered through Whatman No. 1 filter paper and the extract collected in conical flasks. The silver-, copper-, and zinc-mediated nanoparticle synthesis were performed by using the above plant extract. Nanoparticle characterization was conducted using a UV-visible spectrophotometer, X-ray diffraction, and scanning electron microscope (SEM). The antimicrobial potential of eco-friendly produced nanoparticles was investigated. For, $AgNO_3$ mediated synthesis 1 mM $AgNO_3$ (0.1619 g) solution was prepared. Then 10 mL aqueous extract was added to 90 mL of 1 mM $AgNO_3$ solution and kept at 40ºC in dark room for 24 h. The colour change from pale yellow to dark brown was

observed. For $CuSO_4$ mediated synthesis, 1 mM $CuSO_4$ (0.06243 g) solution was prepared and 20 mL aqueous extract added to 80 mL of 1 mM $CuSO_4$ solution which was kept at 45ºC in dark room for 24 h. The colour change from light blue to dark blue depicted the synthesis of Cu nanoparticles. For $ZnSO_4$ mediated synthesis, 1 mM $ZnSO_4$ (0.0288 g) solution was prepared and 20 mL aqueous extract added to 80 mL of 1 mM $ZnSO_4$ solution. It was then kept in dark at 36ºC in dark room for 24 h. The colour change from light yellow to light brown depicted the synthesis of Zn nanoparticles. The above solutions were separately centrifuged at 10,000 rpm for 20 min and the pellets were mixed with petroleum ether for rapid drying. The dried pellets were collected in ethanol in a micro-centrifuge tube and used for characterization and antimicrobial activity assessment.

Characterization of nanoparticles

UV-spectrophotometer analysis*:* Sample suspension (1 mL) was taken in a quartz tube and diluted with 2 mL distilled water to monitor the synthesis of nanoparticles and subsequently scanned in UV-vis spectra between wave lengths of 200-1100 nm in a UV-visible spectrophotometer (Shimadzu UV 1800, Germany). UV-vis spectra were recorded at an interval of 24 h for maximum absorption (Banerjee *et al.,* 2014).

XRD analysis: The purified synthesized nanoparticles were freeze-dried, powered and used for XRD analysis (XRD, Nanopixmini) at 40kv/20 mA using continuous scanning 2 delta mode (Absar *et al.*, 2003). The nanoparticle solution was purified by repeated centrifugation at 5000 rpm for 20 min, followed by redispersion of pellet of nanoparticles into 10 mL deionized water.

SEM analysis of silver nanoparticles

Scanning electron microscopic (SEM) analysis of synthesized nanoparticles was done using VEGA3 TESCAN machine. Thin films of samples were prepared on carbon-coated copper grid by dropping a very small amount of sample on the grid. The extra solution was removed using a blotting paper and then the film on SEM grid were allowed to dry by putting it under a mercury lamp for 5 min.

Antibacterial assay

The test organisms used for antibacterial assay were *Escherichia coli, Pseudomonas aeruginosa, Bacillus subtilis* and *Staphylococcus aureus.* These bacteria were procured from the Department of Zoology, Sri Paramakaliyani Arts and Science College, Alwarkurichi, Tirunelveli (India). The bacterial strains were grown on Muller Hinton (MH) agar plates at 37ºC and maintained on nutrient agar slants. Each organism was maintained in a separate culture medium and recovered for testing by sub-culturing on a fresh medium. Inoculum of each bacterial strain was transferred to 10 mL Muller Hinton agar broth and incubated overnight at 37°C. The antimicrobial activities of synthesized nanoparticles were evaluated by measuring the zone of inhibition as per Bhargav *et al.*, 2016).

Antifungal assay

The standard fungi *Aspergillus flavus* and *Candida albicans*, were collected from the Department of Microbiology, Kamaraj College, Thoothukudi, Tamil Nadu (India) and grown on Sabouraud's dextrose agar (SDA) (Hi Media, India.) at 30°C for 24 and 48 h, respectively. Then 3-5 colonies from each fungus were suspended in 2 mL sterile normal saline and vortexed. The turbidity of homogenous suspension was adjusted to approximately 0.5 McFarland standards (Towers *et al*., 2001). To measure the zone of inhibition the methods og Bhargav et al. (2016) was followed.

Statistical analysis

All the experiments were conducted in triplicate in a completely randomized design The data was presented as mean ± standard error of the mean of the different treatment groups. The data was used to compare more than two groups on the same dependent measure by the analysis of variance (ANOVA). All the statistical test analyses were conducted using Graph Pad Prism 6 software (Nayan and Shukla, 2011).

RESULTS AND DISCUSSION

Synthesis and characterization of nanoparticles

Three types of nanoparticle formation in *H. ficulneus* extract after treatment with different metallic (silver nitrate, copper sulphate and zinc sulphate) aqueous solution. For Ag nanoparticles, the colour changed from yellow to dark brown. In case of Cu nanoparticles, a shift from light blue to dark blue was observed, and for Zn nanoparticles, the colour transitioned from light yellow to light brown occurred. Nanoparticle formations were confirmed through spectral studies, including UV-visible spectroscopy, X-ray diffraction (XRD), and SEM analysis.

UV- visible spectrum analysis of nanoparticles

Reduction of metallic ion to metal nanoparticles during exposure to *H. ficulneus* extract was noticed by colour change. The addition of *H. ficulneus* leaf powder extract to 1 mM silver nitrate solution resulted in the appearance of dark yellow brown solution after 15 min indicating the formation of Ag nanoparticles. Similarly, the addition of *H. ficulneus* leaf powder extract to 1 mM copper sulphate solution lead to the colour change from light blue to dark blue after 20 min indicating the formation of Cu nanoparticles. The addition of *H. ficulneus* leaf powder extract to 1 mM zinc sulphate solution (pale yellow colour) caused colour change to dark brown after 20 min indicating the formation of Zn nanoparticles. The formation of nanoparticles was confirmed UV visible spectroscopy. The colour change observed above was due to the excitation of surface plasmon vibrations (Mulavney, 1996). The broadening of the peak indicated that the particles were poly-dispersed. UV-vis spectroscopy is commonly used to examine the size and shape controlled nanoparticles in aqueous suspensions (Wiley *et al.,* 2006). The presence of nanoparticles was confirmed by obtaining a spectrum in visible range using UV-visible spectrophotometer (Fig. 1).

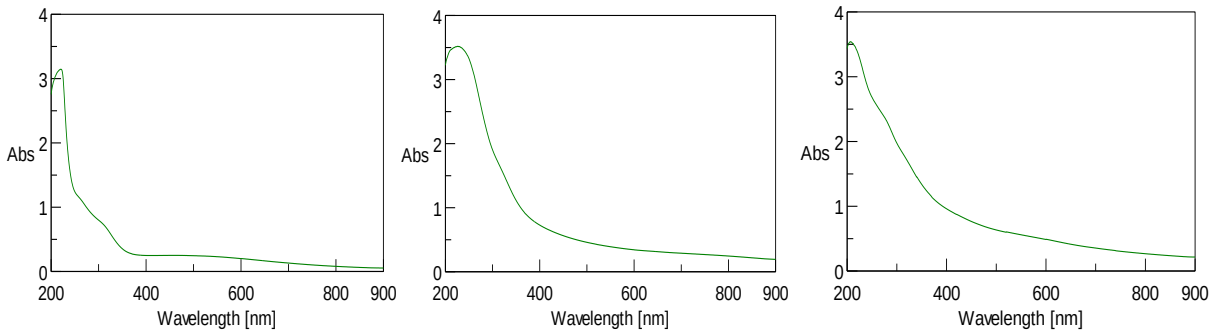

Fig. 1: UV-vis spectra of different nanoparticles of *Hibiscus ficulneus*

The silver-, copper- and zinc-nanoparticle were formed in the peak range of 415, 225 and 260 nm. Absorption spectra of Ag nanoparticles formed in reaction media revealed absorbance peaks in 200-450 nm range; and the absorption peak observed at 415 nm is considered the characteristics peak of Ag nanoparticles. Our findings are supported by Ashokkumar *et al.* (2015) who studied the effect of varying the concentration of leaf extract on the size of Ag nanoparticles. When the surface plasmon vibrations in Ag nanoparticles are excited, the Ag nanoparticles exhibit yellowish brown colour in aqueous solution (Krishnaraj *et al.*, 2010). UV-visible spectroscopy could be used to examine formation of Cu nanoparticles. The absorption spectra of Cu nanoparticles formed in reaction media revealed the absorbance peak in the range of 200 to 400 nm; and the absorption peak observed at 225 nm is the characteristics peak of Cu nanoparticles. UV-vis spectra suggest that sharpness of absorption peak is dependent on concentration ratio of extract (Sheny *et al.,* 2011). The absorption results confirmed the formation of Zn nanoparticles prepared in liquid by bioreduction method. Absorption spectra of Zn nanoparticles formed in reaction media showed the absorbance peak in 200-400 nm range; and the absorption peak at 265 nm is the characteristics peak of Zn nanoparticles.

X-ray diffraction studies

The formation of metallic nanoparticles synthesized by using *H. ficulneus* extracts was confirmed by observing the characteristic peaks during X-ray diffraction (XRD) analysis (Fig. 2-4; Table 1-3) so as to confirm the crystalline nature of nanoparticles. The XRD spectrum of biosynthesized nanoparticles with standard confirmed that the nanoparticles formed were in the form of nanocrystals as evidenced by the peaks at 2θ values.

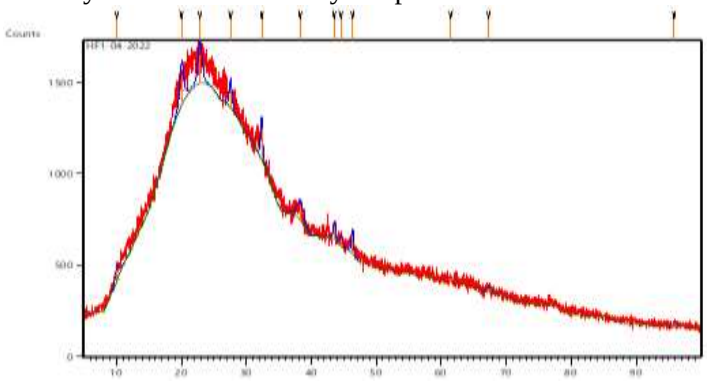

Fig. 2: XRD spectrum of Ag nanoparticles of *H. ficulneus*

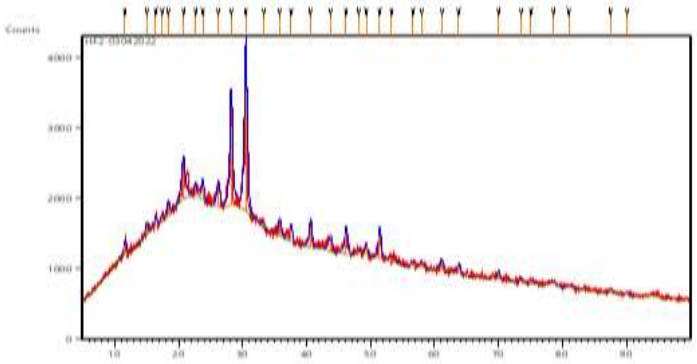

Fig. 3: XRD spectrum of Cu nanoparticles of *H. ficulneus*

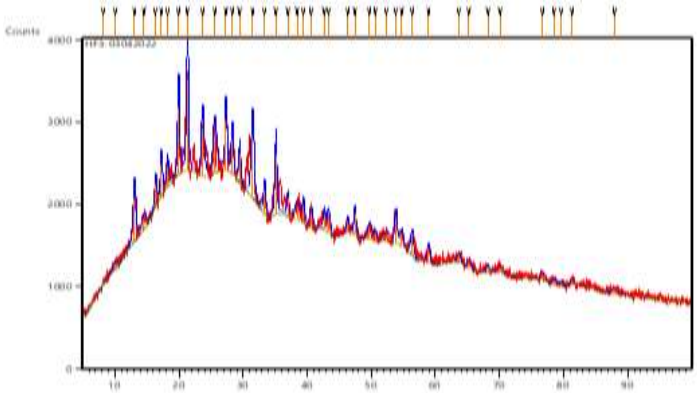

Fig. 4: XRD spectrum of Zn nanoparticles of *H. ficulneus*

The biosynthesized silver nanoparticle produced five characteristic peaks (Fig. 2, Table 1) as observed in the XRD image at 2θ values ranging from 0 to 80Å. The 2θ values of 10.097, 20.030, 22.846, 27.572 and 32.322 were noticed corresponding to the height of 51.71, 161.95, 158.08, 109.19 and 164.55 cts, respectively. The corresponding "d" spacing value of silver nanoparticle were 8.760, 4.432, 3.892, 3.235 and 2.769 Å. The spherical and oval shapes correspond to the state of minimum potential energy. The other factors that play role in determining the shape of Ag nanoparticles are fast reaction rate and low concentration of silver nitrate solution because slower reaction rate and higher concentration of silver nitrate lead to anisotropic Ag nanoparticles (Chandran *et al.*, 2006; Pastoriza-Santos *et al.*, 2008).

The biosynthesized Cu nanostructure produced by using *H. ficulneus* extract yielded nineteen characteristic peaks as observed in XRD image at 2θ values ranging from 0 to 60Å (Fig. 3; Table 2). Comparison of our XRD spectrum with standard confirmed that the Cu nanoparticles formed in our experiments were nanocrystals in form, as evidenced by the peak at 2θ value of 11.689, 15.023, 16.397 and 17.402 corresponding to the height of 141.19, 115.85, 84.88 and 71.47 cts. The corresponding "d" spacing value of Zn nanoparticles was 7.602, 5.897, 5.406 and 5.096Å for synthesized nanoparticles. The biosynthesized zinc nanostructure produced by using *H. ficulneus* extract gave five characteristic peaks in XRD image at 2θ values ranging from 0 to 60Å (Fig. 4; Table 3). A comparison of our XRD spectrum with standard confirmed that the silver particles formed in present study were nanocrystals, as evidenced by the peak at 2θ value of 16.359 corresponding to the height of 14.80, 67.86, 513.51, 121.83 and 265.19 cts. The corresponding "d" spacing value of Zn nanoparticles was 10.801, 8.786, 6.772, 6.084 and 5.418Å. Sathyavathi *et al.* (2014) reported that the XRD pattern had four intense

Table 1: XRD pattern of SNPs & CNPs synthesized by *H. ficulneus* leaf extract with $AgNO_3$ solution

Position [°2θ]	Height [cts]	FWHM left [°2θ]	d-spacing [Å]	RI [%]
10.097	51.71	0.6927	8.760	31.42
20.030	161.95	0.6927	4.432	98.42
22.846	158.08	0.6927	3.892	96.06
27.572	109.19	0.4330	3.235	66.35
32.322	164.55	0.3464	2.769	100.00
38.252	74.30	1.0391	2.352	45.15
43.522	70.16	0.3464	2.079	42.63

SNP: Silver nanoparticles, CNP: Copper nanoparticles, FWHM left: Full width at half maximum left; RI: Reflection intensity

Table 2: XRD pattern of SNPs synthesized by *H. ficulneus* leaf extract with $CuSO_4$ solution

Position [°2θ]	Height [cts]	FWHM left [°2θ]	d-spacing [Å]	RI [%]
11.689	141.19	0.5196	7.602	8.36
15.023	115.85	0.5196	5.897	6.86
16.397	84.88	0.3464	5.406	5.03
17.402	71.47	0.4330	5.096	4.23
18.395	140.40	0.5196	4.823	8.31
20.747	406.00	0.6927	4.281	24.04
22.646	131.61	0.3464	3.926	7.79

SNP: Silver nanoparticles, FWHM left: Full width at half maximum left; RI.: Reflection intensity

Table 3: XRD pattern of SNPs synthesized by *H. ficulneus* leaf extract with $ZnSO_4$ solution

Position [°2θ]	Height [cts]	FWHM left [°2θ]	d-spacing [Å]	RI [%]
8.1855	14.80	0.3464	10.801	1.35
10.067	67.86	0.8659	8.786	6.20
13.072	513.51	0.5196	6.772	46.9
14.558	121.83	0.6927	6.084	11.13
16.359	265.19	0.3464	5.418	24.22
17.257	366.51	0.3464	5.138	33.48
18.224	243.82	0.3464	4.867	22.27

SNP: Silver nanoparticles, FWHM left: Full width at half maximum left; RI: Reflection intensity

peaks in the whole spectrum of 2θ values ranging from 30 to 80 for Ag nanoparticles biosynthesised by *Elaeagnus latifolia* extract suggesting that the crystallization of bio-organic phase occurs on the surface of Ag nanoparticles. Also, the typical XRD pattern revealed that the sample contained a mixed structure of Ag nanoparticles.

SEM analysis of silver nanoparticles

The analysis of scanning electron microscopy (SEM) images predicts the formation and morphology of stable Ag nanoparticles. SEM analysis showed uniform distribution of Ag nanoparticles on the surfaces of cells (Fig. 5). The Ag nanoparticles were spherical in shape with particle size in the range

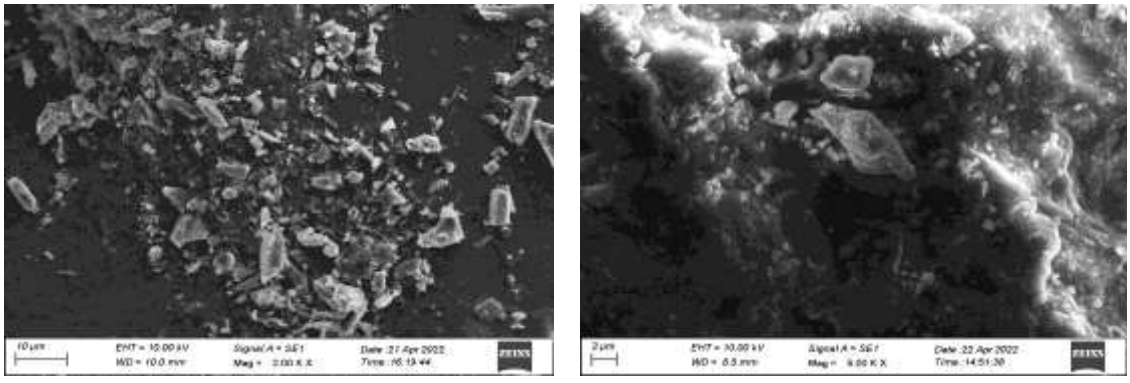

Fig. 5: SEM image of SNPs synthesized by *H. ficulneus* leaf extract with $AgNO_3$ solution

the range of 2 to 20 μm. The larger Ag particles may be due to the aggregation of smaller ones, due to the SEM measurements. SEM analysis showed uniformly distributed Ag nanoparticles on the surfaces of the cells. The colour change to dark orange-brown is due to increased concentration and growth of Ag nanoparticles. After minutes there was no significant colour change confirmed the completion of reduction reaction.

Antimicrobial activity

Infections due to a variety of bacterial etiologic agents such as pathogenic *Escherichia coli, Salmonella* spp., and *Staphylococcus aureus* are most common. The drug resistance to human pathogenic bacteria has commonly been reported all over the world (Mulligen *et al.*, 1996). Plant materials remain an important resource to combat serious diseases in the world. Most plants are medicinally useful in treating human diseases and in most cases the antimicrobial efficacy value attributed to some plants is beyond belief. Conservative estimates suggest that about 10% flowering plants on earth have been used by local communities throughout the world but only 1% have gained recognition. There are about 120 plant-based drugs prescribed worldwide which come from just 95 plant species. The results indicated that different metal nanoparticles have good antimicrobial activity against various microorganisms. Recently, the use of metal nanoparticles against bacteria has increased because of the gradual increase in drug resistance among microorganism (Amin *et al.*, 2012). A number of synthetic drugs have been used to cure various diseases caused by pathogenic microbes in human beings. These drugs produced side effect due to overdose. Several medicinal plants have been used to cure bacterial infection to human beings. In present study antimicrobial activity of *H. ficulneus* against six pathogens is reported and their zone of inhibition is shown in Fig. 6. The antibacterial potential of developed metallic nanoparticles using *H. ficulneus* extracts was carried out by assessing the *in vitro* inhibition of pathogenic bacteria *E. coli, Bacillus subtilis, S. aureus* and *Pseudomonas aeruginosa* (Table 4). Moderate growth inhibition of test pathogens was observed in culture plates as evident from the cleared zones. Maximum zone of inhibition (22 and 20 mm) was noticed in *Ps. aeruginosa* by Ag- and Zn-nanoparticles, respectively, followed by *S. aureus* and *E. coli* (14 mm each) by Ag and Cu nanoparticles, respectively, in comparison to control treatment. *B. subtilis* exhibited least activity (11 mm inhibition zone) in Cu nano particles. The antifungal activity of metallic nanoparticles was carried out against two fungi *viz.*, *Aspergillus flavus* and *Candida albicans*. *A. flavus* and *C. albicans* showed maximum inhibition zone zone (15 mm) in *H. ficulneus* Zn-nanoparticles, whereas *C. albicans* exhibited minimum growth inhibition (11 mm) in Ag nanoparticles (Table 4). Overall, Ag nanoparticles proved better in antibacterial action in comparison to the Zn- or Cu-nanoparticles. The size of metallic nanoparticles ensures that a considerably large surface area of particles is in contact with bacterial cells. Such a large contact outside is predictable to improve the extent of bacterial abolition (Parameswari *et al.*, 2010). Ag nanoparticles have the ability to anchor to the bacterial cell wall and subsequently penetrate it, thereby cause structural changes in cell membrane permeability and cell death. There is

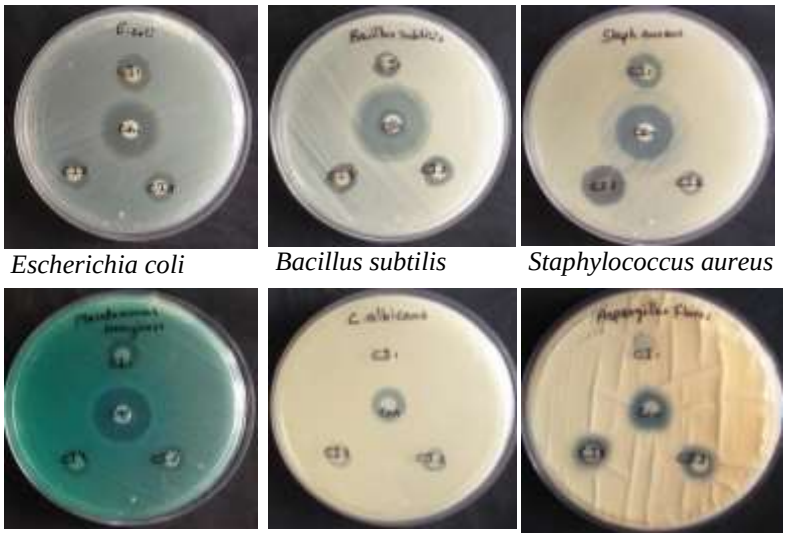

Escherichia coli *Bacillus subtilis* *Staphylococcus aureus*

Ps. Aeruginosa *Candida albicans* *Aspergillus flavus*

Fig. 6: Antimicrobial potential of different nanoparticles of *Hibiscus ficulneus*

Table 4: Antimicrobial potential of different metal nanoparticles of *Hibiscus ficulneus*

Pathogens	Ag nanoparticles ($AgNO_3$)	Cu nanoparticles ($CuSO_4$)	Zn nanoparticles ($ZnSO_4$)	Control (Amikacin)
	Antibacterial activity in terms of zone of inhibition (mm)			
Escherichia coli	12 ± 0.5	14 ± 0.3	13 ± 0.4	23 ± 0.4
Bacillus subtilis	12 ± 0.2	12 ± 0.4	13 ± 0.5	28 ± 0.5
Staphylococcus aureus	14 ± 0.3	11 ± 0.2	13 ± 0.6	24 ± 0.4
Pseudomonas aeruginosa	22 ± 0.4	12 ± 0.5	20 ± 0.4	24 ± 0.3
	Antifungal activity in terms of zone of inhibition (mm)			
Candida albicans	11 ± 0.7	11 ± 0.5	15 ± 0.4	12 ± 0.6
Aspergillus flavus	13 ± 0.2	-	15 ± 0.3	19 ± 0.5

± Standard Error, + Present, - Absent

formation of 'pits' on the cell surface due to the accumulation of nanoparticles on cell surface (Sondi *et al.*, 1969).

Conclusion: The exploitation of bioprocess products is currently receiving considerable attention, driving a technological revolution in pharmacological field. Among the various methods for synthesizing natural products, chemical reduction and green synthesis have garnered significant attention due to their ability to precisely control particle size and morphology. Notably, NMR plays a pivotal role in the analysis of nanoparticles, and their wide-ranging applications in diverse fields hold promise for future research.

Acknowledgement: The authors are thankful to the Management and Principle of GVN College (Autonomous) for their support and providing infrastructure to conduct this research.

Author's contribution: AS: Framing study design and experimentation. Data analysis and drafting of manuscript. AS and NSJ assisted in experiments. IK proofread and reviewed the manuscript. All the authors reviewed the manuscript.

Conflict of interests: All the authors declare that they have no competing interests.

Ethical statement: This study does not involve any active human participants.

REFERENCES

Absar, A., Shankar, S. and Murali, S. 2003. Geranium leaf biosynthesis of silver nanoparticles. *Biotechnology Progress*, **19**: 1627-1631.

Amin, M., Anwar, F., Janjua, M.R.S.A., Iqbal, M.A. and Rashid, U. 2012. Green synthesis of silver nanoparticles through reduction with *Solanum xanthocarpum* L. Berry extract: Characterization, antimicrobial and urease inhibitory activities against *Helicobacter pylori*. *International Journal of Molecular Sciences*, **13**(8): 9923-9941.

Ashokkumar, S., Ravi, S., Kathiravan, V. and Velmurugan, S. 2015. Synthesis of silver nanoparticles using *A. indicum* leaf extract and their antibacterial activity. *Spectrochimica Acta. Part A: Molecular and Biomolecular Spectroscopy*, **134:** 34-39.

Baishya, D., Sharma, N. and Bora, R. 2012. Green synthesis of silver nanoparticle using *Bryophyllum pinnatum* (Lam.) and monitoring their antibacterial activities. *Archives of Applied Science Research*, **4(**5): 2-7.

Banerjee, P., Satapathy, M., Mukhopahayay, A. and Das, P. 2014. Leaf extract mediated green synthesis of silver nanoparticles from widely available Indian plants: Synthesis,

characterization, antimicrobial property and toxicity analysis. *Bioresources and Bioprocessing*, **1**(3): 1-5.

Bhargav, H.S., Shastri, S., Purushothama, P.S., Darshan K.M. and Nayak, M. 2016. Measurement of the zone of inhibition of an antibiotic. pp. 409-414. **In**: *Conference: 2016 IEEE 6th International Conference on Advanced Computing (IACC)* [DOI:10.1109/IACC.2016.82].

Buzea, C., Pacheco, I.I. and Robbie, K. 2007. Nanomateriales and nanoparticles: Sources and toxicity. *Biointerphases*, **2**(4): [MR17–MR71. [doi:10.1116/1.2815690].

Chandran, S.P., Chaudhary, M., Pasricha, R., Ahmad, A. and Sastry, M. 2006. Synthesis of gold nanotriangles and silver nanoparticles using *Aloe vera* plant extract. *Biotechnology Progress*, **22**(2): 577-583.

Dickson, R.M. and Lyon, L.A. 2000. Unidirectional plasmon propagation in metallic nanowires. *Journal of Physical Chemistry B*, **104**(26): 6095-6098.

Fonnegra, F.G. 2007. *Plantas medicinales aprobadas en Colombia*. University of Antioquia, Antioquia, Colombia.

Joppa, L.N., Roberts, D.L., Myers, N. and Pimm, S.L. 2011. Biodiversity hotspots house most undiscovered plant species. *Proceedings of the National Academy of Sciences (USA*, **108**(32): 13171-13176.

Kavitha, K.S., Baker, S., Rakshith, D., Kavitha, H.U., Rao, Y.H.C., Harini, B.P. and Satish, S. 2013. Plants as green source towards synthesis of nanoparticles. *International Research Journal of Biological Sciences*, **2**(6): 66-76.

Krishnaraj, C., Jagan, E.G., Rajasekar, S., Selvakumar, P., Kalaichelvan, P.T. and Mohan, N. 2010. Synthesis of silver nanoparticles using *Acalypha indica* leaf extracts and its antibacterial activity against water borne pathogens. *Colloids and Surfaces. B, Biointerfaces*, **76**(1): 50-56.

Mulligen, A.N., Schaefer, H. and Lahaye, R. 1993. Evaluation of candidate DNA bar-coding loci for economically important timber species of the mahogany family (Meliaceae). *Molecular Ecology Resources*, **11***:* 450-460.

Mulvaney, P. 1996. Surface plasmon spectroscopy of nanosized metal particles. *Langmuir*, **12**(3): 788-800.

Murugan, A. and Shanmugasundaram, K.K. 2014. Biosynthesis and characterization of silver nanoparticles using the aqueous extract of *Vitex negundo* L. *World Journal of Pharmacy and Pharmaceutical Sciences*, **3**(8): 1385-1393.

Nayan, R., Bhalodia and Shukla, V.J. 2011. Antibacterial and antifungal activities from leaf extracts of *Cassia fistula* L.: An ethnomedicinal plant. *Journal of Advanced Pharmaceutical Technology & Research*, **2**(2): 104-109.

Pandey, M.M., Rastogi, S. and Rawat, A.K.S. 2008. Indian herbal drug for general healthcare: An overview. *Internet Journal of Alternative Medicine*, **6**(1): 3 [*https://ispub.com/IJAM/6/1/10275*].

Parameswari, E., Udayasoorian, C., Sebastian, S.P. and Jayabalakrishnan, R.M. 2010. The bactericidal potential of silver nanoparticles. *International Research Journal of Biotechnology*, **1**(3): 44-49.

Pastoriza-Santos, I. and Liz-Marzán, L.M. 2008. Colloidal silver nanoplates. State of the art and future challenges. *Journal of Materials Chemistry*, **18**(15): 1724-1737.

Patwardhan, B., Warude, D., Pushpangadan, P. and Bhatt, N. 2005. Ayurveda and traditional Chinese medicine: A comparative overview. *Evidence-Based Complementary and Alternative Medicine*, **2**(4): 465-473.

Pimm, S.L., Jenkins, C.N., Abell, R., Brooks, T.M., Gittleman, J.L., Joppa, L.N. and Sexton, J.O. 2014. The biodiversity of species and their rates of extinction, distribution, and protection. *Science*, **344(**6187): 1-10.

Sathyavathi, G.S., Ganesh, D., Kumar, S.J.U., Senthilkumar, U., Newmaster, S.G., Ragupathy, S. and Ravikanth, G. 2014 Assessing product adulteration in natural health products for laxative yielding plants, *Cassia, senna*, and *Chamaecrista*, in Southern India using DNA barcoding. *International Journal of Legal Medicine*, **129:** 693-700.

Sheny, D.S., Mathew, J. and Philip, D. 2011. Phytosynthesis of Au, Ag and Au-Ag bimetallic nanoparticles using aqueous extract and dried leaf of *Anacardium occidentale*. *Spectrochimica Acta. Part A: Molecular and Biomolecular Spectroscopy*, **79**(1): 254-262.

Sondi, A.B., Raut. and Quimby, M.W. 1969. False negative saponins test results induced by the presence of tannins. *Lloydia*, **32**: 52-58.

Towers, G.H., Lopez, A. and Hudson, J.B. 2001. Antiviral and antimicrobial activities of medicinal plants. *Journal of Ethnopharmacology*, **77**: 189-196.

Wang, E., Qi, X., Xing, M., Zhao, W. and Chen, X. 2000. Rhizosphere and non-rhizosphere bacterial community composition of the wild medicinal plant *Rumex patientia*. *World Journal of Microbiology and Biotechnology*, **28**: 2257-2265.

Wiley, B.J., Im, S.H., Li, Z.Y., McLellan, J., Siekkinen, A. and Xia, Y. 2006. Maneuvering the surface plasmon resonance of silver nanostructures through shape-controlled synthesis. *Journal of Physical Chemistry. B*, **110**(32): 15666-15675.

Yuan, H., Ma, Q., Ye, L. and Piao, G. 2016. The traditional medicine and modern medicine from natural products. *Molecules*, **21**(5): 559. [*doi:10.3390/molecules21050559*].